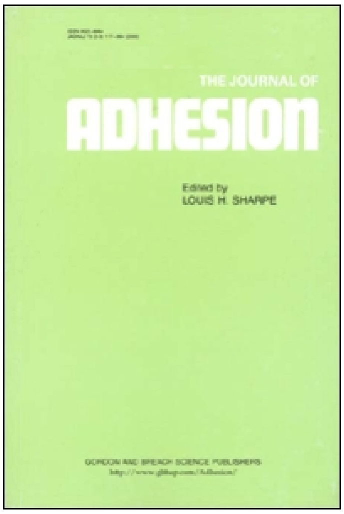

The Journal of Adhesion
Publication details, including instructions for authors and subscription information:
http://www.informaworld.com/smpp/title~content=t713453635

Mode II Fracture Toughness of a Brittle and a Ductile Adhesive as a Function of the Adhesive Thickness

Lucas F. M. da Silva[a]; F. A. C. R. G. de Magalhães[a]; F. J. P. Chaves[b]; M. F. S. F. de Moura[a]
[a] Departamento de Engenharia Mecânica, Faculdade de Engenharia da Universidade do Porto, Porto, Portugal [b] Instituto de Engenharia Mecânica (IDMEC), Porto, Portugal

Online publication date: 02 September 2010

To cite this Article da Silva, Lucas F. M. , de Magalhães, F. A. C. R. G. , Chaves, F. J. P. and de Moura, M. F. S. F.(2010) 'Mode II Fracture Toughness of a Brittle and a Ductile Adhesive as a Function of the Adhesive Thickness', The Journal of Adhesion, 86: 9, 891 — 905

To link to this Article: DOI: 10.1080/00218464.2010.506155

URL: http://dx.doi.org/10.1080/00218464.2010.506155

The Journal of Adhesion, 86:891–905, 2010

ISSN: 0021-8464 print/1545-5823 online
DOI: 10.1080/00218464.2010.506155

Mode II Fracture Toughness of a Brittle and a Ductile Adhesive as a Function of the Adhesive Thickness

Lucas F. M. da Silva[1], F. A. C. R. G. de Magalhães[1], F. J. P. Chaves[2], and M. F. S. F. de Moura[1]
[1]Departamento de Engenharia Mecânica, Faculdade de Engenharia da Universidade do Porto, Porto, Portugal
[2]Instituto de Engenharia Mecânica (IDMEC), Porto, Portugal

The main goal of this study was to evaluate the effect of the thickness and type of adhesive on the Mode II toughness of an adhesive joint. Two different adhesives were used, Araldite ® AV138/HV998 which is brittle and Araldite 2015 which is ductile. The end notched flexure (ENF) test was used to determine the Mode II fracture toughness because it is commonly known to be the easiest and widely used to characterize Mode II fracture. The ENF test consists of a three-point bending test on a notched specimen which induces a shear crack propagation through the bondline. The main conclusion is that the energy release rate for AV138 does not vary with the adhesive thickness whereas for Araldite 2015, the fracture toughness in Mode II increases with the adhesive thickness. This can be explained by the adhesive plasticity at the end of the crack tip.

Keywords: Adhesive thickness; Brittle adhesive; Ductile adhesive; End notched flexure test; Epoxy; Mode II fracture toughness

1. INTRODUCTION

Adhesively bonded joints were initially designed using a continuum mechanics approach. The maximum principal stress was proposed for very brittle materials whose failure mode is normal to the direction of maximum principal stress [1,2]. However, because of the singularity of stresses at the re-entrant corners of joints, the stresses depend on the mesh size used and how close to the singular points the stresses

Received 22 February 2010; in final form 7 May 2010.
Address correspondence to Lucas F. M. da Silva, Departamento de Engenharia Mecânica, Faculdade de Engenharia da Universidade do Porto, Rua Dr. Roberto Frias, 4200-460 Porto, Portugal. E-mail: lucas@fe.up.pt

are taken. Therefore, care must be exercised when using this criterion. When ductile adhesives are used, criteria based on maximum stress are not appropriate because such joints can still carry large loads after adhesive yielding. For ductile adhesives, Adams and Harris [2] used maximum principal strain as the failure criterion for predicting joint strength. Hart-Smith [3] proposed that the maximum adhesive shear strain might be used as a failure criterion when plastic deformation of the adhesive occurred. da Silva *et al.* [4] implemented this criterion into a commercial software package. Other analyses go beyond that of Hart-Smith, by taking into consideration both shear and peel contributions to plasticity, such as that of Adams and Mallick [5]. More recently, da Silva *et al.* [6,7] have shown for single lap joints that the maximum shear strain criterion is very accurate for ductile adhesives.

Continuum mechanics assumes that the structure and its material are continuous. Defects or two materials with re-entrant corners obviously violate such an assumption. Consequently, continuum mechanics gives no solution at these singular points because of the stress or strain singularities. Cracks are the most common defects in structures, for which the method of fracture mechanics has been developed. In linear elastic fracture mechanics (LEFM), it is well accepted that stresses calculated by using continuum mechanics are singular (infinite) at the crack tip. Although LEFM is mainly used for dealing with sharp cracks, angular wedged notches are also of practical importance. The use of a generalized stress-intensity factor, analogous to the stress-intensity factor in classical LEFM, to predict fracture initiation for bonded joints at the interface corners has been investigated [8–10]. Damage mechanics has been used to model the progressive damage and failure of a pre-defined crack path [11–14]. The damage is confined to a zero volume line or a surface and the procedure is often referred to as a cohesive zone model (CZM). A CZM simulates the fracture process, extending the concept of continuum mechanics by including a zone of discontinuity modelled by cohesive zones, thus using both local strength and energy parameters to characterize the debonding process. This allows the approach to be of much more general utility than conventional fracture mechanics.

In order to apply a fracture mechanics or damage mechanics approach, it is necessary to have the fracture toughness of the material. The fracture toughness varies with the type of loading, *i.e.*, Modes I, II, III, and mixed. Most of the data available in the literature is for the fracture toughness in Mode I using the double cantilever beam. However, adhesive joints are also loaded in Mode II and under mixed mode. For the determination of the toughness in Mode II there are various test methods available (Fig. 1): the end notched flexure (ENF) test, the end loaded split (ELS) test, and the four-point notched flexure (4ENF) test. The ELS test presents large displacements and is sensitive to the clamping device. The 4ENF is more sophisticated but has problems of friction due to the loading mode in the pre-crack region. The easier and probably most common testing method for Mode II is the ENF test. The ENF test consists of a three-point bending test on a pre-cracked specimen causing a shear mode loading in the adhesive.

It is known that the adhesive toughness varies with the adhesive thickness, especially with ductile adhesives because of the constraining effects of the adherends. The thickness of the adhesive layer

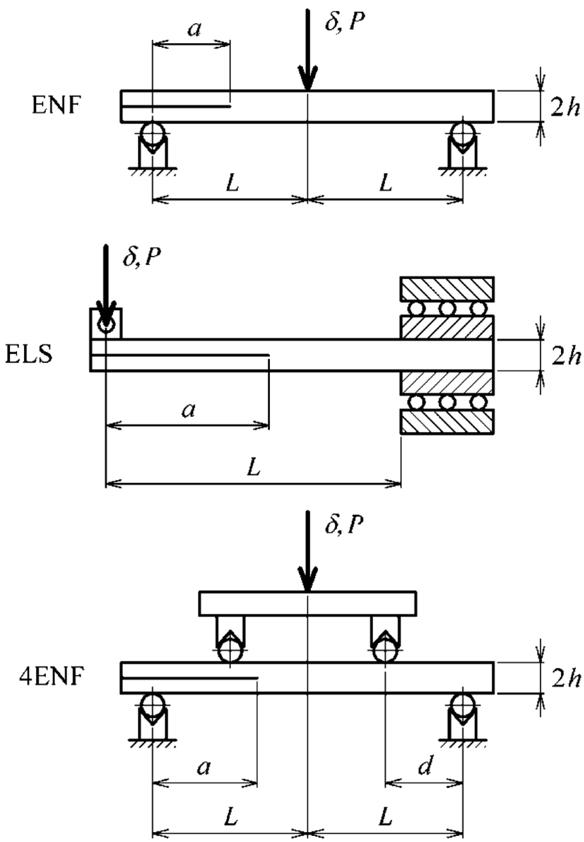

FIGURE 1 Schematic representation of the end notched flexure (ENF) test, end loaded split (ELS) test, and four-point notched flexure (4ENF) test methods.

contributes to the joint behaviour. Thus, it should be taken into account and thoroughly studied. Bascom *et al.* [15,16] found that fracture energy is maximized when the adhesive layer thickness equals that of the fracture process zone (FPZ) ahead of the crack tip. Kinloch and Shaw [17] showed that the FPZ played an important role in enhancing G_{Ic} of the adhesive joint. Daghyani *et al.* [18,19] found a transition in the fracture process from a cohesive to an interfacial adhesive failure for thin layers. Lee *et al.* [20] found that as bond thickness decreases, the fracture energy either decreases monotonically, or increases, peaks, and then decreases rapidly. Most of the results in the literature concerning the effect of the adhesive thickness are for Mode I, but little is available concerning Mode II, which should be the main loading mode in adhesive joints.

The main objective of the present study was to measure the Mode II fracture toughness of two types of adhesive (brittle and ductile) using the ENF test as a function of the adhesive thickness.

2. EXPERIMENTAL DETAILS

2.1. Materials

Two adhesives were selected, a very stiff and brittle epoxy (AV138/HV998 from Huntsman, Salt Lake City, UT, USA) used in aerospace applications, and a more flexible and ductile epoxy adhesive (2015 from Huntsman). Table 1 shows the shear properties of the adhesives used in this work. The properties were determined using the thick adherend shear test [21].

The heat-treated steel DIN 40CrMnMo7 was used for the substrates. It is a high strength steel with a yield strength of 900 MPa that is sufficient to keep the material in the elastic range.

2.2. Specimen Geometry

The specimen geometry is represented in Fig. 2. The geometry used for the ENF test is the one used for the double cantilever beam test where

TABLE 1 Adhesive Shear Properties Using the Thick Adherend Shear Test Method ISO 11003-2 [21]

	AV138 M/HV998	2015
Shear modulus G (MPa)	1559 ± 11	487 ± 77
Shear yield strength τ_{ya} (MPa)	25.0 ± 0.55	17.9 ± 1.80
Shear strength τ_r (MPa)	30.2 ± 0.40	17.9 ± 1.80
Shear failure strain γ_f (%)	5.50 ± 0.44	43.9 ± 3.40

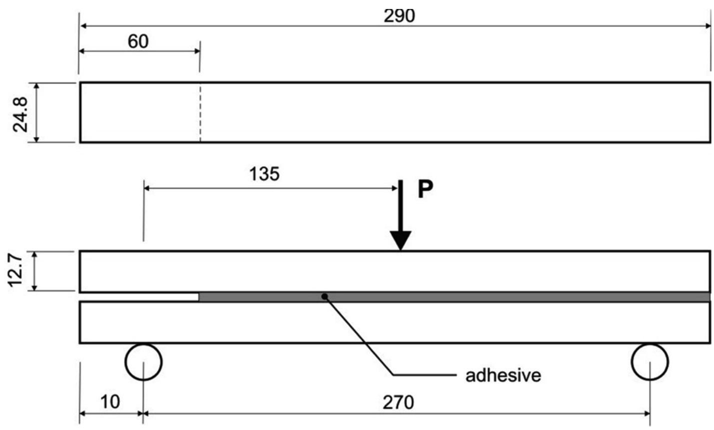

FIGURE 2 Geometry of the end notched flexure (ENF) test specimen (dimensions in mm).

the adherend thickness, h, is 6.35 mm. The length between the supports, $2L$, was 270 mm and the initial crack length was 50 mm. Three adhesive thicknesses were studied for each adhesive: 0.2, 0.5, and 1 mm.

2.3. Specimen Manufacture

The joint surfaces were grit blasted with corundum (600 μm particles) under a pressure of 6 bar and degreased with acetone prior to the application of the adhesive. The resin and hardener of the brittle epoxy AV138/HV998 were mixed manually and applied with a spatula on the substrates. The ductile epoxy 2015 was mixed with a nozzle and applied directly on the surfaces. Spacers were inserted between the adherends before the application of the adhesive in order to control the bondline thickness. These spacers were removed after the adhesive was cured. Joints with AV138/HV998 were cured for 16 h at 45°C and those with 2015 were cured for 6 h at 45°C. A sharp pre-crack in the adhesive layer mid-thickness was assured using a razor blade and a gentle tap. To guarantee the correct pre-crack position at the adhesive layer middle plane, a simple set with a razorblade glued in between two feeler gauges was introduced in the gap between the upper and lower adherends to promote the pre-crack. This set was done with a 0.1-mm thick razorblade glued in between two feeler gauges with half the bond line thickness minus 0.05 mm to account for the razorblade thickness. A jig with spacers for the correct alignment of the adherends was used and is shown in Fig. 3. It was verified in a previous study [22] that friction effects in the ENF test

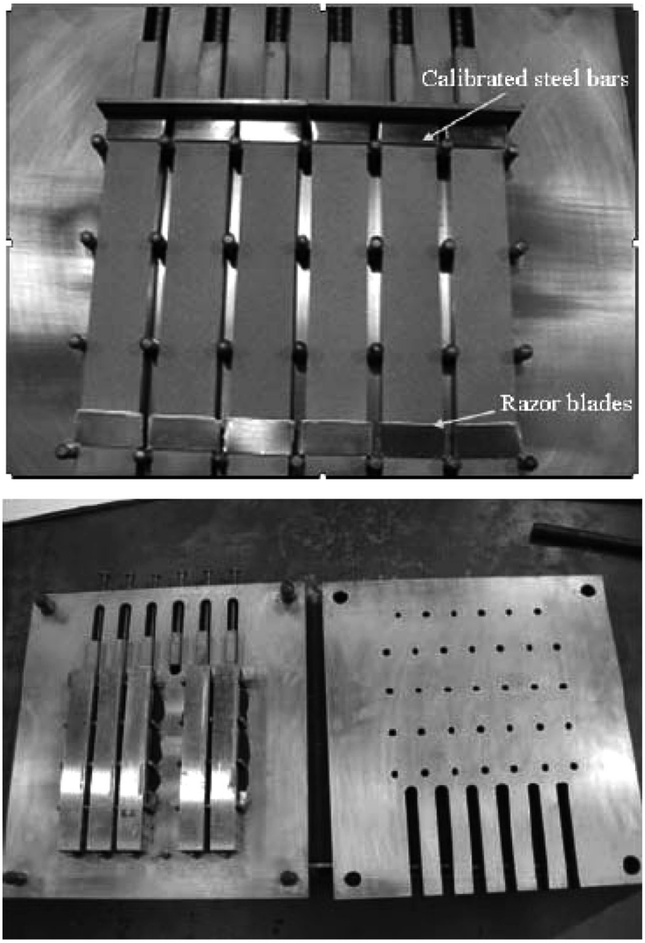

FIGURE 3 End notched flexure specimen fabrication (shims for bondline thickness control at the top and assembled specimens in a jig at the bottom).

are mainly concentrated at the region of the pre-crack above the support. Consequently, two sheets of Teflon® with a thin pellicle of lubricator between them were included in the pre-crack region in order to minimize friction effects.

2.4. Testing

The ENF specimens were tested in laboratory conditions (~25°C and ~50% relative humidity) using a universal testing machine, under a constant crosshead rate of 0.25 mm/min. The load–displacement

(P–δ) curve was registered during the test. Despite the difficult identification of the crack tip in Mode II testing, pictures were recorded during the testing of the specimens at 5 s intervals using a 10 MPixel digital camera. This procedure allows measuring the crack length during its growth and afterwards collecting the P–δ–a parameters. This was performed correlating the time elapsed from the beginning of each test between the P–δ curve and each picture (the testing time of each P–δ curve point is obtained accurately with the absolute displacement and the established loading rate). The specimens were marked with a white paint and a ruler to facilitate the crack length (a) reading. Three specimens were tested for each configuration.

2.5. Data Analysis

According to linear elastic fracture mechanics [23],

$$G_c = \frac{P_c^2}{2b}\frac{dC}{da}, \tag{1}$$

where C is the compliance defined by $C = \delta/P$, P_c is the load for crack growth, and b is the joint width. According to beam theory and using Eq. (1),

$$G_{IIc} = \frac{9P_c^2 a^2}{16b^2Eh^3}, \tag{2}$$

where G_{IIc} is the toughness in Mode II. The toughness in Mode II can also be determined by finding the partial derivative of the compliance with crack length using an analytical equation (usually a cubic polynomial) that fits the experimental data of the compliance *versus* the crack length. However, in any case, the experimental measurement of the crack length is very laborious because the two substrates are against each other and make the identification of the crack tip very difficult. Also, the crack tip the fracture process zone (FPZ), where damage of the material occurs by plasticisation and micro-crackling, absorbs part of the energy. Therefore, an equivalent crack length (a_e) that takes into account the FPZ should be used. To overcome these two problems (crack monitoring and FPZ), de Moura and Morais [24] proposed a method that does not require the crack length measurement and that takes into account the FPZ that they called the compliance-based beam method (CBBM). Using beam theory and accounting for the shear effects, the following equation is obtained

$$C = \frac{3a^3 + 2L^3}{12EI} + \frac{3L}{10Gbh}. \tag{3}$$

In this equation, the crack length does not include the effects of energy dissipation at the FPZ and the moduli E and G refer only to the adherends. However, it is expected that the compliance of the adhesive, and its thickness, can influence the global compliance of the specimen. Consequently, an equivalent flexural modulus can be estimated considering the initial compliance, C_0, and the initial crack length, a_0:

$$E_f = \frac{3a_0^3 + 2L^3}{12I}\left(C_0 - \frac{3L}{10Gbh}\right)^{-1}. \tag{4}$$

On the other hand, the effect of the FPZ on the compliance can be included through an equivalent crack length (a_e), which is the sum of the real crack length (a) are the correction (Δa_{FPZ}) induced by the presence of the FPZ:

$$C = \frac{3(a + \Delta a_{FPZ})^3 + 2L^3}{12E_f I} + \frac{3L}{10Gbh}. \tag{5}$$

Combining Eqs. (5) and (4), the equivalent crack length can be obtained as a function of the current measured compliance:

$$a_e = a + \Delta a_{FPZ} = \left[\frac{C_{corr}}{C_{0corr}}a_0^3 + \frac{2}{3}\left(\frac{C_{corr}}{C_{0corr}} - 1\right)L^3\right]^{1/3}, \tag{6}$$

where C_{corr} and C_{0corr} are given by

$$C_{corr} = C - \frac{3L}{10Gbh}; \quad C_{0corr} = C_0 - \frac{3L}{10Gbh}.$$

Substituting the value of a_e in Eq. (2),

$$G_{II} = \frac{9P^2}{16b^2E_f h^3}\left[\frac{C_{corr}}{C_{0corr}}a_0^3 + \frac{2}{3}\left(\frac{C_{corr}}{C_{0corr}} - 1\right)L^3\right]^{2/3}. \tag{7}$$

This method does not require crack length monitoring during crack growth which was observed to be very difficult to perform with accuracy in the ENF test. Moreover, it provides an R-curve as a function of the equivalent crack length, thus allowing a clear identification of the fracture energy from its plateau.

3. RESULTS

3.1. Brittle Adhesive (AV138)

All the specimens failed cohesively in the adhesive, as shown in Fig. 4. Representative experimental P–δ curves of the ENF specimens for

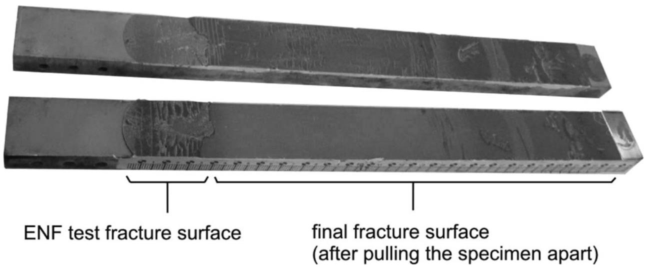

FIGURE 4 Failure surfaces of end notched flexure (ENF) specimens with the brittle adhesive AV138.

each adhesive thickness are presented in Fig. 5. The curves are linear to failure which is in accordance with the brittle nature of the adhesive. The crack propagation occurred suddenly after the maximum load. An experimental *R*-curve obtained for an adhesive thickness of 0.5 mm is shown in Fig. 6. *R*-curves are used to identify the fracture energy from the plateau corresponding to the self-similar crack propagation. A plateau barely appears because the adhesive is brittle and leads to an unstable crack propagation. Figure 7 shows the values of G_{IIc} as a function of the adhesive thickness. The brittle adhesive AV138 is not sensitive to the adhesive thickness and gives an approximately constant value of 5 N/mm. The fracture toughness was determined using the compliance-based beam method (CBBM) because it was not possible to monitor the crack during its growth due to the sudden and unstable crack propagation.

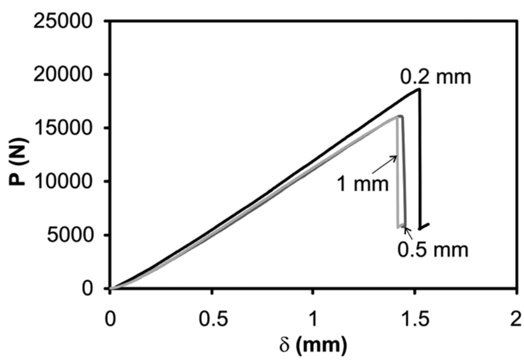

FIGURE 5 Representative experimental P–δ curves of the ENF specimens with the brittle adhesive AV138 as a function of the adhesive thickness.

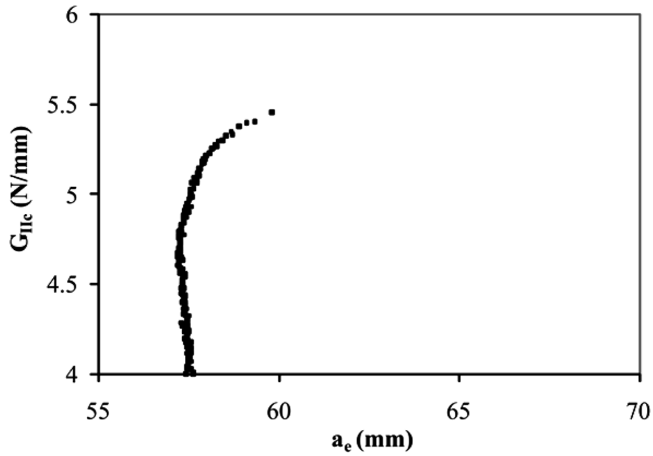

FIGURE 6 Typical experimental *R*-curve obtained for the brittle adhesive AV138 for a thickness of 0.5 mm.

3.2. Ductile Adhesive (2015)

All the specimens failed cohesively in the adhesive, as shown in Fig. 8. Representative experimental P–δ curves of the ENF specimens for each adhesive thickness are presented in Fig. 9. In this case, the curves are non-linear corresponding to the plastic deformation of the adhesive. An experimental *R*-curve obtained for an adhesive thickness of 0.5 mm is shown in Fig. 10. A plateau is clearly seen indicating

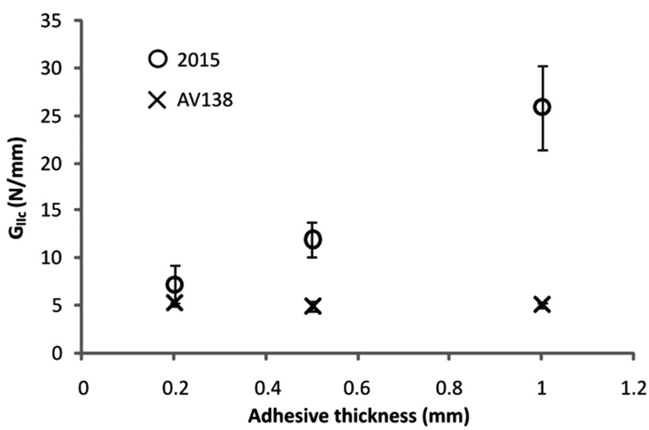

FIGURE 7 Mode II fracture toughness (G_{IIc}) as a function of the adhesive thickness for a ductile adhesive (2015) and a brittle adhesive (AV138).

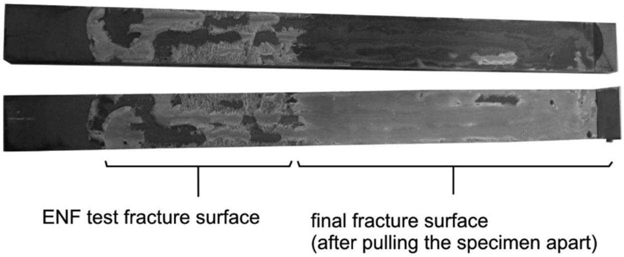

FIGURE 8 Failure surfaces of ENF specimens with the ductile adhesive 2015.

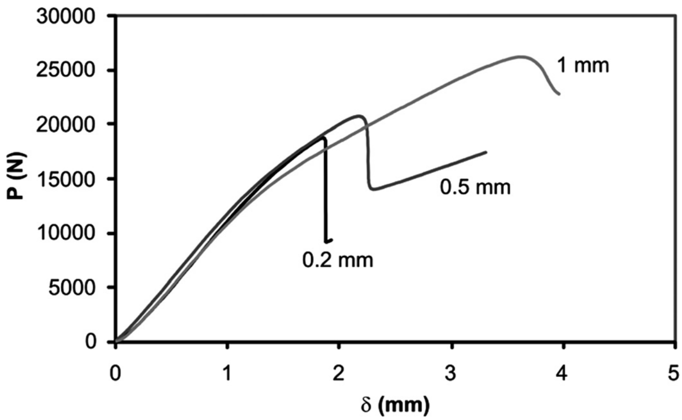

FIGURE 9 Representative experimental P–δ curves of the ENF specimens with the ductile adhesive 2015 as a function of the adhesive thickness.

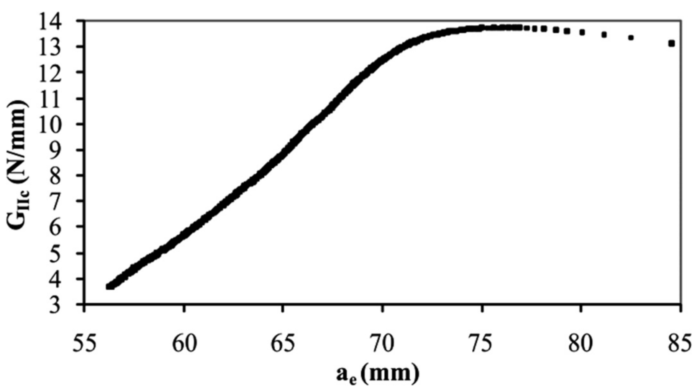

FIGURE 10 Typical experimental R-curve obtained for the ductile adhesive 2015 for a thickness of 0.5 mm.

TABLE 2 Fracture Toughness in Mode II (G_{IIc}) Determined Using the Beam Theory and the CBBM Method for the Ductile Adhesive 2015 (Only One Specimen Used for Each Adhesive Thickness)

Adhesive thickness (mm)	Beam theory G_{IIc} (N/mm)	CBBM G_{IIc} (N/mm)
0.5	11.3	13.2
1	21.2	32.4

stable crack propagation. Figure 7 shows the values of G_{IIc} as a function of the adhesive thickness. The fracture toughness in Mode II increases with the adhesive thickness. The values presented in Figure 7 were obtained using the CBBM method. However, in the case of the 2015 adhesive, it was possible to measure the crack length and determine the fracture toughness using beam theory. Table 2 shows that the beam theory underestimates the G_{IIc}, especially for large bondline thicknesses (0.5 and 1 mm).

4. DISCUSSION

In adhesive bonding it is important to understand that the adhesive layer applied in between the two bonded bodies is usually thin (of the order 0.05 to 0.2 mm for the aeronautical industry and up to 1 mm or more for the civil industry); thus, it behaves differently compared with the adhesive as a bulk material. If it is true that thicker adhesive layers result in bad joint properties, when the adhesive layer becomes thinner than the surface roughness it is difficult for the adhesive to promote the connection between the two surfaces because there are points where the two adherends come into contact. The ability to absorb energy, characterizing ductile or brittle adhesives, also plays an important role when evaluating the bondline thickness effect. The explanation for the results presented above is probably linked with the FPZ size. Although no measurements of the FPZ were performed in this work, it is known that in the case of a brittle adhesive, the FPZ is negligible and probably the adherends do not interfere with the strain energy release rate measured. However, in the case of the ductile adhesive 2015, the results give the idea that the fracture toughness measured is influenced by the adhesive thickness, since this parameter decisively influences the natural FPZ development, as shown schematically in Fig. 11. The value of G_{IIc} used for modelling purposes to design an adhesive joint should be that measured in

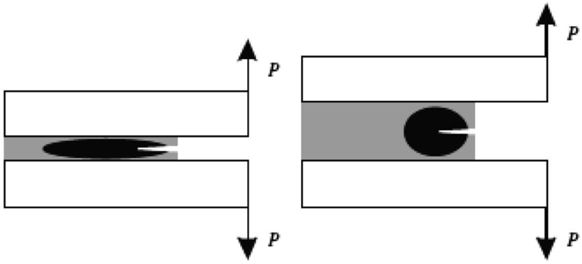

FIGURE 11 Fracture process zone (FPZ) as a function of the adhesive bondline thickness.

a fracture mechanics joint with the same adhesive thickness. This aspect is often not taken into account and may lead to erroneous results.

The strain energy release rate measured here in Mode II can be compared with that measured in Mode I by the same authors in another paper [25]. The fracture toughness in Mode I was measured using the double cantilever beam method under a test speed similar to that used in the present analysis and under the same ambient conditions. The adhesive thickness that was used is 0.5 mm. The values are presented in Table 3 along with the Mode II values and the relation G_{IIc}/G_{Ic}. It is common in the literature to assume a value of 2 for G_{IIc}/G_{Ic} when the value of G_{IIc} is unknown [24,26]. However, the results presented here show that the value can be much higher. Therefore, it is important to test not only in Mode I but also in Mode II for the true adhesive properties. Another study [27] has shown a value of approximately 10 for G_{IIc}/G_{Ic} for adhesive 2015 but for an adhesive thickness of 0.2 mm. This reinforces the fact that the adhesive toughness to be used for simulation purposes should use properties determined in conditions similar to those found in the real structure.

TABLE 3 Comparison of the Fracture Toughness in Mode I (G_{Ic}) and Mode II (G_{IIc}) for an Adhesive Thickness of 0.5 mm (Average Values)

Adhesive	G_{Ic} (N/mm) [24]	G_{IIc} (N/mm) (present study)	G_{IIc}/G_{Ic}
Brittle (AV138)	0.346	4.91	14.2
Ductile (2015)	0.526	11.9	22.6

5. CONCLUSIONS

The fracture toughness in Mode II (G_{IIc}) was measured using the ENF test for a brittle adhesive (AV138) and a ductile adhesive (2015) using three adhesive thicknesses (0.2, 0.5, and 1 mm). The following conclusions can be drawn:

1. The critical strain energy release rate (G_{IIc}) for the brittle adhesive AV138 does not vary with the adhesive thickness and is approximately 5 N/mm.
2. The critical strain energy release rate (G_{IIc}) for the ductile adhesive (2015) increases with the adhesive thickness, varying from 7.15 N/mm for 0.2 mm to 25.8 N/mm for 1 mm.
3. The different behaviour between the two types of adhesives can be explained by the fracture process zone (FPZ) ahead of the crack tip. In the case of the brittle adhesive, that FPZ is negligible in contrast to the case of the ductile adhesive which interferes with the adherends.
4. The relation G_{IIc}/G_{Ic} for the adhesives studied here is of at least one order of magnitude.

REFERENCES

[1] Adams, R. D. and Peppiatt, N. A., *J. Strain Anal.* **9**, 185–196 (1974).
[2] Adams, R. D. and Harris, J. A., *Int. J. Adhes. Adhes.*, **4**, 65–78 (1984).
[3] Hart-Smith, L. J., Adhesive-bonded single-lap joints, NASA Contract Report, Hampton, Virginia, NASA CR-112236 (1973).
[4] da Silva, L. F. M., Lima, R. F. T., and Teixeira, R. M. S., *J. Adhesion* **85**, 889–918 (2009).
[5] Adams, R. D. and Mallick, V., *J. Adhesion* **38**, 199–217 (1992).
[6] da Silva, L. F. M., das Neves, P. J. C., Adams, R. D., and Spelt, J. K., *Int. J. Adhes. Adhes.* **29**, 319–330 (2009).
[7] da Silva, L. F. M., das Neves, P. J. C., Adams, R. D., Wang, A., and Spelt J. K., *Int. J. Adhesion Adhesives* **29**, 331–341 (2009).
[8] Xu, J.-Q., Liu, Y.-H., and Wang, X.-G., *Engineering Fracture Mechanics* **63** (6), 775–790 (1999).
[9] Groth, H. L., *Int. J. Adhes. Adhes.* **8**, 107–113 (1988).
[10] Gleich, D. M., Van Tooren, M. J. L., and Beukers, A., *J. Adhesion Sci. Technol.* **15** (9), 1091–1101 (2001).
[11] Duan, K., Hu, X., and Mai, Y.-W., *J. Adhesion Sci. Technol.* **18** (1), 39–54 (2004).
[12] Needleman, A., *J. Applied Mechanics* **54**, 525–531 (1987).
[13] Ungsuwarungsri, T. and Knauss, W. G., *Int. J. Fracture* **35**, 221–241 (1987).
[14] Tvergaard, V. and Hutchinson, J. W., *J. Mechanics and Physics of Solids* **40**, 1377–1397 (1992).
[15] Bascom, W. D., Cottington, R. L., Jones, R. L., and Peyser, P., *J. Appl. Polym. Sci.* **19**, 2545–2562 (1975).
[16] Bascom, W. D. and Cottington, R. L., *J. Adhesion* **7**, 333–346 (1976).

[17] Kinloch, A. J. and Shaw, S. J., *J. Adhesion* **12**, 59–77 (1981).
[18] Daghyani, H. R., Ye, L., and Mai, Y. W., *J. Adhesion* **53**, 149–162 (1995).
[19] Daghyani, H. R., Ye, L., and Mai, Y. W., *J. Adhesion* **53**, 163–172 (1995).
[20] Lee, D., Ikeda, T., Miyazaki, N., and Choi, N., *J. Engineering Materials and Technology* **126**, 14–18 (2004).
[21] Marques, E. A. S. and da Silva, L. F. M., *J. Adhesion* **84**, 917–936 (2008).
[22] Silva, M. A. L., de Moura, M. F. S. F. and Morais, J. J. L. *Composites: Part A* **37**, 1334–1344 (2006).
[23] Irwin, G. R., *Appl. Mater. Res.* **3**, 65–81 (1963).
[24] de Moura, M. F. S. F. and de Morais, A. B., *Eng. Fract. Mech.* **75**, 2584–2596 (2008).
[25] da Silva, L. F. M., Carbas, R. J. C., Critchlow, G. W., Figueiredo, M. A. V., and Brown, K., *Int. J. Adhes. Adhes.* **29**, 621–632 (2009).
[26] da Silva, L. F. M., Rodrigues, T. N. S. S., Figueiredo, M. A. V., de Moura, M. F. S. F., and Chousal, J. A. G., *J. Adhesion* **82**, 1091–1115 (2006).
[27] Campilho, R. D. S. G., de Moura, M. F. S. F., Ramantani, D. A., Morais, J. J. L., and Domingues, J. J. M. S., *Int. J. Adhes. Adhes.* **29**, 678–686 (2009).